Polyhedron 45 (2012) 23–29

Contents lists available at SciVerse ScienceDirect

Polyhedron

journal homepage: www.elsevier.com/locate/poly

Structural and dynamic NMR characterization of $[Pd(bipy)(R\text{-thiourea})_2]^{2+}$ and $[Pd(phen)(R\text{-thiourea})_2]^{2+}$ cations

Archimede Rotondo *, Salvatore Barresi, Matteo Cusumano, Enrico Rotondo

Dipartimento di Chimica Inorganica, Analitica e Chimica Fisica, Università di Messina, Italy

ARTICLE INFO

Article history:
Received 5 April 2012
Accepted 8 July 2012
Available online 27 July 2012

Keywords:
Palladium(II)–thiourea complexes
^1H, ^{13}C, ^{15}N NMR
Dynamics
Conformational analysis

ABSTRACT

The synthesis and characterization of 10 complexes, $[Pd(bipy)(R\text{-TU})_2]Cl_2$ and $[Pd(phen)(R\text{-TU})_2]Cl_2$ (bipy = 2,2′-bipyridyl; phen = 1,10-phenanthroline; *R*-TU = N-alkyl substituted thioureas), is presented. The conformational and dynamic behavior in solution, analyzed by several NMR techniques, is compared to that of the free thiourea ligands. Spectra at variable temperatures of the free thioureas are consistent with hampered rotation around the C–N bonds. Mono-alkyl derivatives, in methanol, show equilibria between *syn* and *anti* conformers, whereas di-alkyl thioureas show equilibria between the *syn–anti* and *syn–syn* conformers (*syn* and *anti* indicate the position of the alkyl chain with respect to the S atom over the two amino-branches). *Syn* protons of the alkyl-chains are converted into the corresponding *anti* protons by C–N rotation, which also exchanges external (close to the S atom) to internal N–H (on the opposite side with respect to the S atom) within the NMR timescale. This is also observed for the corresponding Pd^{II} complexes, which, according to the enhancement of the double C–N bond character, present slower *syn*/*anti* exchanges. Moreover, metal coordination selects *anti* conformers for the mono-alkyl thioureas, and *syn–anti* conformers for the di-alkyl thioureas.

1. Introduction

Pt^{II} and Pd^{II} thioureate complexes have been widely studied because of the peculiar hydrogen bonding networks that are able to build up specific solid state structures [1,2]. These are also tunable by specific counter-ions [3] or solvents [4], driving to different metal–thiourea conformational arrangements which are new building blocks for crystal structures. The presence of two N and one S donor atom makes thioureas potential multidentate ligands, as shown in some papers concerning the formation of metallacages [5,6]. On another hand, because of the known anti-cancer activity of several Pt based drugs [7], complexes containing d^8 metal–sulfur bonds have become crucial. Indeed, already in the blood, where Pt drugs are injected or infused, S-donor ligands are strong competitors for the metal coordination sites [8,9]. In this contest Pt-sulfur adducts could act as drug reservoirs and/or reduce metal drug toxicity [10–12]. Therefore the wide interest on the kinetic behavior of these complexes is not surprising, especially with respect to nucleophilic substitution [13–16]. Among d^8 metal complexes targeting DNA as intercalators, some thioamido species are mentioned and have been carefully studied [17,18]; whereas a few years ago our group focused on the synthesis and characterization of Pd^{II} and Pt^{II} complexes bearing flat ligands, such as 2,2′-bipyridyl (bipy) or 1,10-phenanthroline (phen), with demonstrated intercalation abilities, and S-apto-alkyl substituted thioureas [19,20]. The important role of the ancillary thioamidic ligands is also witnessed by the pharmacological activity of similar Pt^{IV} species, claimed to be pro-drugs undergoing reduction to the Pt^{II} active analogs in cancer cells [21–23]. In this paper we present the synthesis, characterization and dynamic behavior of new $[Pd(bipy)(R\text{-TU})_2]Cl_2$ and $[Pd(phen)(R\text{-TU})_2]Cl_2$ complexes (*R*-TU = N-alkyl substituted thioureas). Our studies are addressed toward pseudo biological conditions so that our data can be related to the assessed pharmacological activity.

2. Material and methods

2.1. Physical measurements

^1H, $^{13}C\{^1H\}$ and $^{15}N\{^1H\}$ NMR spectra of the ligands and their analogous complexes were obtained on a Bruker Avance 300 MHz NMR spectrometer operating at frequencies of 300.13, 75.47 and 30.42 MHz, respectively. The main results were also checked on a Varian 500 MHz spectrometer operating at 499.74, 125.73 and 50.65 Mz, respectively, for the mentioned nuclei. The five free thiourea species (**1**–**5**) were analyzed in $CDCl_3$ and CD_3OH, whereas the corresponding Pd^{II} complexes have been investigated in several media; the main results are reported in CD_3OH and

* Corresponding author. Address: Dipartimento di Chimica Inorganica, Analitica e Chimica Fisica, Università di Messina, Via Stagno D'Alcontres 31, Vill. S. Agata-98166, Messina, Italy. Tel.: +39 090 6765729.
E-mail address: arotondo@unime.it (A. Rotondo).

0277-5387/$ - see front matter © 2012 Elsevier Ltd. All rights reserved.
http://dx.doi.org/10.1016/j.poly.2012.07.064

Table 1
^{1}H NMR cs assigned to the resonances shown by the thiourea derivates (**1**–**5**) in CD_3OH at 260 K (245 K where specified).

Code	H-α_s	H-β_s	H-γ_s	H-δ_s	H-α_a	H-β_a	H-γ_a	H-δ_a	$NH_{s(int)}$	$NH_{a(ext)}$	NH_{2int}	NH_{2ext}
TU **1**	–	–	–	–	–	–	–	–	–	–	7.22	7.36
meTU **2**	2.97^s	–	–	–	2.78^a	–	–	–	7.61^s	7.87^a	7.35^a 7.00^s	7.62^a 7.00^s
n-buTU **3**	3.47^s	1.56^s	1.39^s	0.96^s	3.12^a	1.52^a	1.37^a	0.96^a	7.73^s	7.80^a	7.39^a 6.85^s	7.49^a 6.85^s
dietTU **4***	3.58^{sa} 3.49^{ss}	1.14^{sa}	–	–	3.14^{sa}	1.14^{sa}	–	–	7.61^{sa} 7.19^{ss}	7.56^{sa}	–	–
dibuTU **5***	3.53^{sa} 3.47^{ss}	1.55^{sa} 1.53^{ss}	1.35^{sa}	0.94^{sa}	3,10^{sa}	1.51^{sa}	1.35^{sa}	0.94^{sa}	7.62^{sa} 7.22 ^{ss}	7.55^{sa}	–	–

$*$ = cs at 245 K; s = signal coming from the *syn* conformer; a = signal coming from the *anti* conformer; ss = signal coming from the *syn–syn* conformer; sa = signal coming from the *syn–anti* conformer. Isomeric percentage ratios of *syn*/*anti* forms are 41:59 and 56:44 for **2** and **3** respectively. The isomeric percentage *syn–syn*/*syn–anti* ratio is 34:66 and 40:70 for **4** and **5** respectively. Where not reported, there is signal overlap between the conformational isomers.

Table 2
^{13}C and ^{15}N NMR cs assigned to the resonances shown by thiourea derivates (**1**–**5**) in CD_3OH at 260 K (245 K where specified).

Code	C=S	C-α_s	C-β_s	C-γ_s	C-δ_s	C-α_a	C-β_a	C-γ_a	C-δ_a	^{15}NHs	^{15}NHa	^{15}NH2
TU **1**	183.7	–	–	–	–	–	–	–	–	–	–	105.2
meTU **2**	180.1^a 183.8^s	30.7^s	–	–	–	29.0^a	–	–	–	101.0 ^{s}	105.2 ^{s}	103.7^a 100.2^s
n-buTU **3**	179.4^s 183.0^a	44.4 ^{s}	31.1 ^{s}	19.8 ^{s}	12.9 ^{s}	43.1^a	30.2^a	19.7^a	12.8^a	115.3^s	118.6^a	102.7^a 99.7^s
dietTU **4**$*$	178.4^{sa} 182.1^{ss}	39.7^{sa} 38.7^{ss}	14.1^{sa} 13.7^{ss}	–	–	37.2^{sa}	12.6^{sa}	–	–	117.7^{sa} 113.6^{ss}	116.1^{sa}	–
dibuTU **5**$*$	178.8^{sa} 182.5^{ss}	44.7^{sa} 43.7 ^{ss}	31.5^{sa} 31.2^{ss}	19.8	13.0	42.2 ^{sa}	30.2 ^{sa}	19.8 ^{sa}	12.9 ^{sa}	115.0 ^{sa} 110.6^{ss}	113.5^{sa}	–

$*$ = cs at 245 K; s = signal coming from the *syn* conformer; a = signal coming from the *anti* conformer; ss = signal coming from the *syn–syn* conformer; sa = signal coming from the *syn–anti* conformer. Where not reported, there is signal overlap between the conformational isomers.

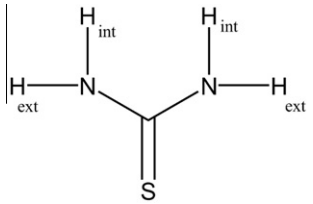

Scheme 1. Labelling of H atoms for thiourea.

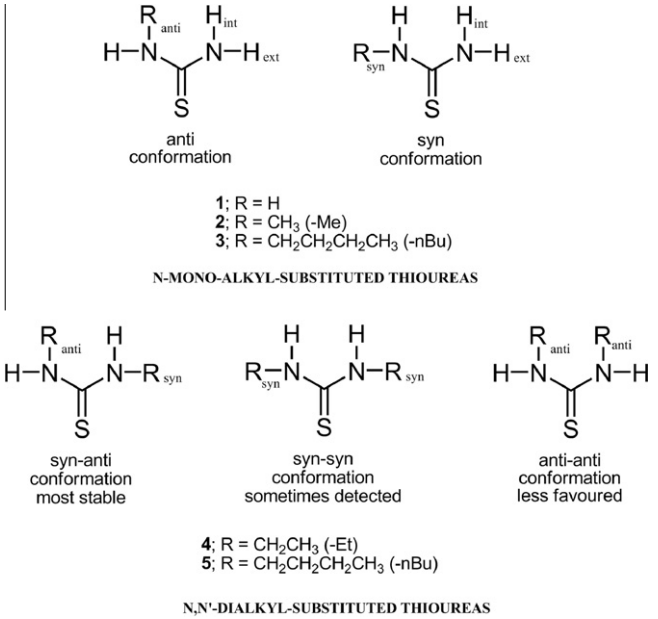

Scheme 2. Molecular conformation and labeling for **1**–**5**.

water/acetone-d_6 80:20 v:v (just to check possible anomalous media effects). In these solvents it is possible both to check out the important N–H signals for complexes in a quasi biological environment and to observe the low temperature (*lt*) behavior of these systems. Chemical shift (cs) of the free ligands and the corresponding complexes are reported in Tables 1 and 2, respectively. We have chosen to present the ^{1}H, ^{13}C and ^{15}N cs in CD_3OH at 260 K because these are optimal conditions to compare and evaluate all the reported resonances. Calibration was attained using the residual proton signal of the solvent ([D_3]methanol: δ = 3.33 ppm) and the ^{13}C solvent septuplet (δ = 47.7 ppm) as internal standards. ^{15}N calibration was referred to CH_3NO_2 as an external standard (90% CH_3NO_2 in CD_3OH: δ = 380.5 ppm). For **4** and **5**, we had to report cs at lower temperatures (245 K) because of fast exchange (Fig. 3). Variable temperature spectra were run to fully characterize the chemical species and to gain thermodynamic information about the conformational changes of these systems. Thermodynamic data coming from these measurements are reported in the "Results and Discussion" section.

The pH measurements were performed with a Metrohm 827 pHlab pH-meter equipped with a 3 mm electrode to measure the pH inside the NMR tubes. Conductivity measures were performed with a Metrohm 712 bridge.

2.2. Syntheses and characterizations of ***1a–5a*** and ***1b–5b***

Palladium(II) chloride ($PdCl_2$), 2,2′-bipyridine (bipy), 1,10-phenanthroline (phen), thiourea (TU, **1**), N-methylthiourea (meTU, **2**), N-buthylthiourea (buTU, **3**), N,N′-diethylthiourea (dietTU, 4) and N,N′-dibuthylthiourea (dibuTU, **5**) were purchased as pure reagents at AG, from Sigma Aldrich. Potassium tetrachloropalladate(II) was prepared by the reaction of palladium chloride with a slight excess of potassium chloride. The complexes [Pd(bipy)Cl_2] and [Pd(phen)Cl_2], were obtained by adding 1 mmol of the respective ligand to 0.326 g (1 mmol) of K_2[$PdCl_4$] suspended/dissolved in 40 mL of wet methanol under reflux for about 1 h. The precipitated crystalline powders were recovered by filtration and dried under

vacuum for 2 h. 0.25 mmol of these complexes (83 and 89 mg, respectively) were then suspended again in a water/methanol mixture, whereupon 0.5 mmol of the respective thiourea (**1–5**) was added under reflux. After 1 h, clear yellow to orange solutions were obtained. These solutions were filtrated and the filtrates were kept for 3–5 days at room temperature for crystallization. As a result yellow–red crystals were obtained. The experimental yield of the products, based on Pd, was more than 50%. All the solvents, of analytical grade, were dried and deoxygenated before being used. Elemental analyses were performed at the Microanalytical Laboratory of Redox snc (Milano). Characterization details are extensively quoted in the supplementary material.

2.3. Free activation energy

The free activation energy was calculated, at coalescence, using the Eyring equation ($\Delta G^{\#} = -RT\ln(k_B T/hk)$). The variance in $\Delta G^{\#}$ (Var $\Delta G^{\#}$) was calculated as Var $\Delta G^{\#} = (RT)^2\{[\Delta T/T(\ln(Tk_B/hk)+1)]^2 + (\Delta k/k)^2\}$ with a determination uncertainty of the temperature ΔT of 2 *K* and a relative determination uncertainty of the rate constant $\Delta k/k$ of 0.1 [24]. The $\Delta G^{\#}$ uncertainty is ±1 kJ/mol.

3. Results and discussion

Structural and dynamic behavior of $[Pd(bipy)(R\text{-}TU)_2]^{2+}$ (**1a–5a**) and $[Pd(phen)(R\text{-}TU)_2]^{2+}$ cations (**1b–5b**) give rise to interest because of their important biological activity [19,20]. On the basis of a rough perpendicular arrangement of the thiourea planar moiety with respect to the metal coordination plane, several isomeric solid state structures arise due to hampered rotation about the C–N, C–S and/or S–M bonds [1–4,25]. However conformational dynamics are expected in solution where, so far, less information was available. To achieve this objective, we performed a preliminary study of the five free thioureas (Schemes 1 and 2), so that data could be compared to those of the corresponding Pd^{II} complexes (Scheme 3).

3.1. NMR characterization of the free thioureas

Unsubstituted thiourea (N_2H_4CS, **1**) in CD_3OH at *rt* shows the NH_2 protons as a broad signal split at 260 K into two broad singlets due to internal and external N–H environments (Scheme 1). This is proved by a H_{int}/H_{ext} crosspeak connection in either 2D-TOCSY and 2D-NOESY spectra (scalar and dipolar couplings). Moreover

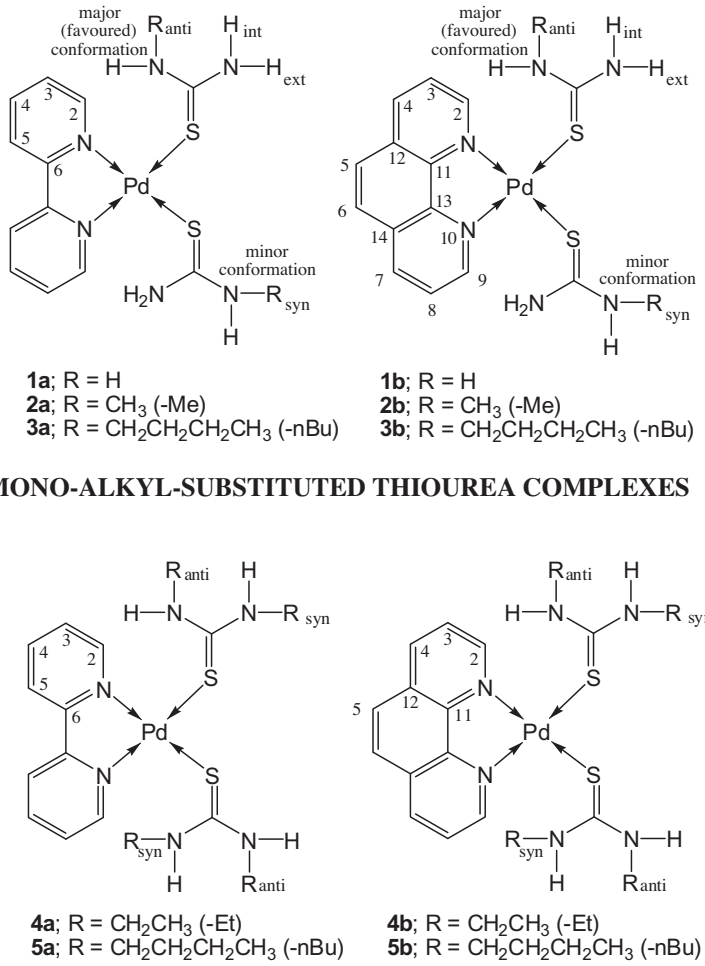

Scheme 3. Representation and numbering/labeling scheme for **1a–5a** and **1b–5b**. Charges are omitted. We have termed *anti*- or *syn*-complexes, the substrates bearing the alkyl chain *syn* or *anti* with respect to the S atom. N–H labels, for the sake of clarity, are either *external* or *internal* if placed on the same side or on the opposite side with respect to the S atom, respectively.

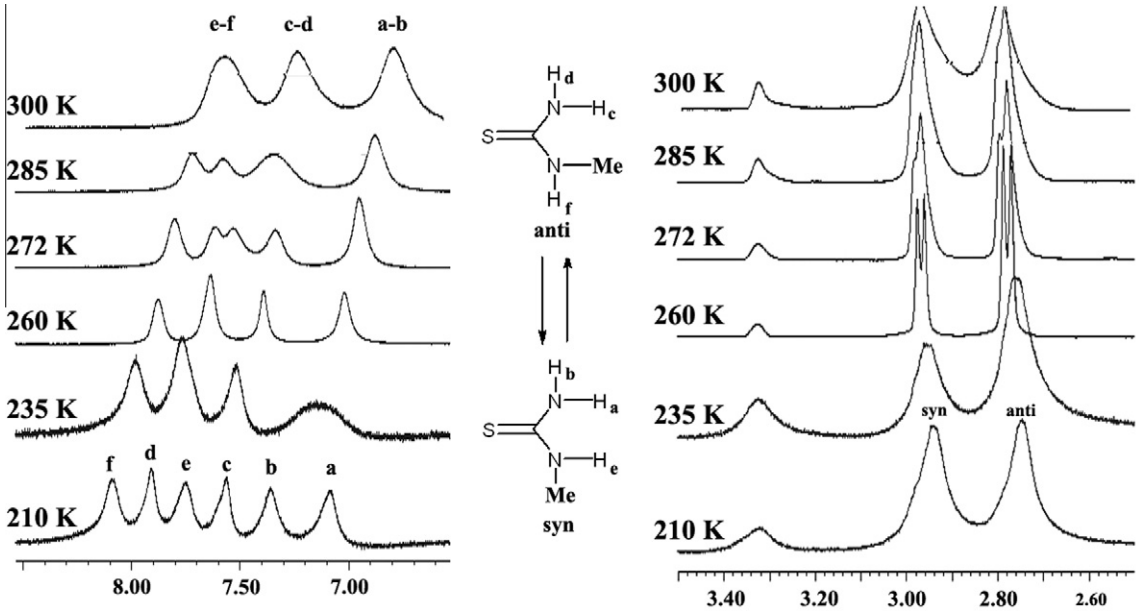

Fig. 1. Variable temperature profile of the regions of interest for N-methyl-thiourea **2**: the schematic assignment (at 260 K) highlights the presence of two exchanging conformers.

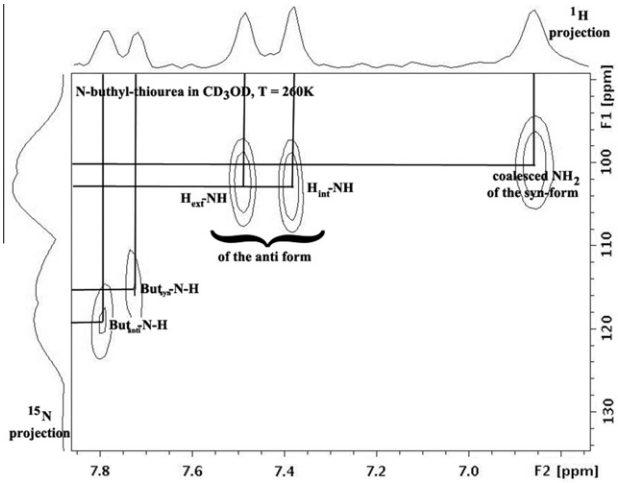

Fig. 2. ^{15}N–^{1}H HSQC 2D-spectrum of **3** in CD_3OH at 260 K with spot assignment of both *syn* and *anti* conformers.

^{1}H–15N HSQC show both signals connected with the same ^{15}N resonance. Mono-alkyl thioureas (**2** and **3**, Scheme 2), because of the locked rotation about the C–N bond, show at 260 K two geometric isomers, namely *syn* and *anti*, according to the orientation of the alkyl substituent, being either on the same side or on the other side with respect to the S atom, respectively (Scheme 2, Fig. 1). Although the thermodynamic stabilities of these conformers in CD_3OH are comparable, spectra in $CDCl_3$ at 260 K demonstrate the *anti* isomer is more stable (the *syn*/*anti* integration intensity ratio is about 3:1). In CD_3OH at 260 K, the N–H protons of the *anti* form arise as three different resonances with a 1:1:1 integration ratio. As evidenced by the ^{15}N-HSQC (Fig. 2), it is possible to assign the R–N–H proton and the two distinct *internal* and *external* protons attached to the same $^{15}NH_2$ nucleus (Figs. 1 and 2). The *syn* isomer at 260 K shows, in the NH region, only two peaks with a 1:2 integration ratio, being the NH_2 protons at coalescence. At 210 K this resonance is split by C–NH_2 rotational freezing (Figs. 1 and 2S). The spectra by themselves indicate that the activation energy of the C–NH_2 rotation is significantly increased by hindering provoked by the internal alkyl position (*anti* form, Fig. 1). Actually, H–N–H proton exchange takes place through two possible mechanisms: (i) C–NH_2 rotation; (ii) solvent mediated acid–base exchange. Quantitative 2D-EXSY and saturation transfer experiments show that, below *rt*, the acid–base mechanism is negligible with respect to the rotational exchange, which however becomes increasingly important above *rt*. Free dialkyl thioureas (**4** and **5**), because of the hampered rotation about the C–N bond, could give rise to three isomeric conformations: *syn–syn, anti–anti* and *syn–anti* (Scheme 2). In $CDCl_3$, the clear presence, at *lt*, of two sets of ^{1}H, ^{13}C and ^{15}N resonances with the same signal intensity connected through chemical exchange suggests the *syn–anti* conformer overwhelms the other arrangements. NOESY/ROESY cross-peaks evidencing through-space contacts unambiguously confirm the unique presence the *syn–anti* form. In CD_3OH, *lt* resonances splitting is consistent with the presence of a *syn–anti*/*syn–syn* equilibrium taking place within the NMR timescale (Scheme 1, Fig. 3). The *anti–anti* isomer was never detected, either in $CDCl_3$ or in CD_3OH.

3.2. Characterization of the Pd^{II} complexes

Coordination to Pd^{II} (Scheme 3) does not change the main profile of the thiourea NMR signals (they are slightly shifted toward higher frequencies, Tables 3 and 4). A significant consequence of complexation is an increase of the C–N rotational barrier which leads to a clear conformational resolution up to *rt* (Figs. 4 and 5). 1-D NMR spectra show an apparent C_2v symmetry due to the lack of significant magnetic influence of the *syn* or *anti* arrangement on the frequencies of the twin ligand. In other words, the thiourea resonances of these complexes perceive just the local symmetry, regardless of the conformation of the *cis* ligand.

Deep spectroscopic analysis concerning the mono-alkyl complexes allowed the complete assignment of both the most populated *anti* and the less populated *syn*-conformer. Evidence of space contacts confirm that the *internal* HN–H is close to both the geminal *external* HN–H and the *anti* α-alkyl protons; whereas the external HN–H and RN–H protons show space proximity only

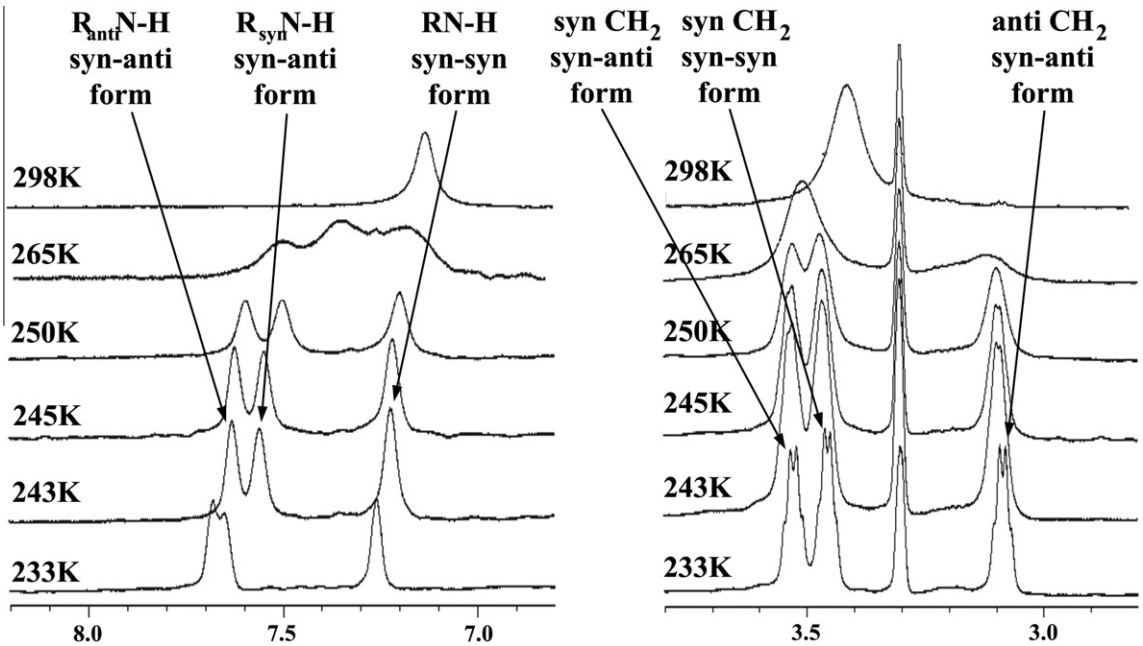

Fig. 3. Variable temperature profile of the main region for N,N′-dibuthylTU **5** in CD_3OD.

Table 3
^{1}H cs of Pd^{II} complexes **1a**–**5a** and **1c**–**5c** in CD_3OH at 260 K.

Code	H-2	H-3	H-4	H-5	H-α_s	H-β_s	H-γ_s	H-δ_s	H-α_a	H-β_a	H-γ_a	H-δ_a	NH_s (int)	NH_a (ext)	NH_{2int}	NH_{2ext}
1a	9.20	7.84	8.36	8.62	–	–	–	–	–	–	–	–	–	–	8.14	8.83
1b	9.47	8.15	8.95	8.29	–	–	–	–	–	–	–	–	–	–	8.18	8.89
2a	9.16	7.82	8.35	8.61	3.13^s	–	–	–	2.86	–	–	–	8.84	9.17	8.30	9.05
2b	9.40	8.13	8.94	8.27	3.20^s	–	–	–	2.87	–	–	–	n.d.	9.27	8.36	9.12
3a	9.17	7.82	8.35	8.62	3.58^s	1.66^s	1.53^s	1.00^s	3.21	1.55	1.34	0.93	8.93^s	9.20	8.30	8.98
3b	9.35	8.10	8.91	8.24	3.63^s	1.71^s	1.47^s	1.03^s	3.22	1.54	1.33	0.92	8.67^s	9.28	8.32	9.03
4a	9.01	7.81	8.36	8.62	3.69	1.32	–	–	3.30	1.13	–	–	8.58	9.18	–	–
4b	9.14	8.05	8.86	8.19	3.71	1.33	–	–	3.25	1.06	–	–	8.57	9.21	–	–
5a	9.07	7.81	8.35	8.62	3.64	1.70	1.41	1.01	3.25	1.51	1.30	0.89	8.55	9.13	–	–
5b	9.19	8.07	8.87	8.21	3.70	1.76	1.48	1.07	3.23	1.47	1.25	0.87	8.58	9.26		

s = resonances coming from the less abundant *syn* form, which is 10%, 15%, 10% and 8% of the *anti* isomer for **2a**, **2b**, **3a** and **3b** respectively. Complexes **4a**, **4b**, **5a** and **5b** are only in the *syn–anti* conformation.

Table 4
^{13}C and ^{15}N cs of Pd^{II} complexes **1a**–**5a** and **1b**–**5b** in CD_3OH at 260 K.

Code	C-2	C-3	C-4	C-5	C-12	C-11 C-6	C=S	C-α_s	C-β_s	C-γ_s	C-δ_s	C-α_a	C-β_a	C-γ_a	C-δ_a	^{15}NHs	^{15}NHa	^{15}NH2
1a	149.3	127.0	141.3	123.3	–	156.6	179.0	–	–	–	–	–	–	–	–	–	–	108.8
1c	149.7	125.7	140.4	127.6	131.1	147.0	177.3	–	–	–	–	–	–	–	–	–	–	109.0
2a	149.2	127.2	141.3	123.7	–	156.6	173.6	31.3^s	–	–	–	29.5	–	–	–	111.9^s	110.4	107.9
2c	149.6	125.7	140.3	127.5	131.0	146.7	173.5	33.4^s	–	–	–	29.5	–	–	–	n.d.	110.8	108.2
3a	149.2	127.2	141.3	123.5	–	156.6	172.7^a 175.0^s	43.5^s	30.2^s	19.8^s	12.7^s	43.8	29.9	19.6	12.6	125.3^s	123.0	107.4
3c	149.6	127.6	140.3	125.7	131.0	146.8	172.6	45.0^s	31.2	19.9	13.0	43.7	30.0	19.7	12.8	n.d	124.1	107.7
4a	149.4	127.3	141.3	123.9	–	156.7	171.4	40.4	14.2	–	–	38.0	12.5	–	–	119.0	125.7	–
4c	149.7	125.7	127.6	140.2	131.0	146.8	171.3	40.4	14.2	–	–	37.9	12.4	–	–	118.8	125.9	–
5a	149.4	127.2	141.3	123.8	–	156.6	171.3	45.2	31.8	18.9	13.1	42.7	30.3	19.7	12.9	116.5	123.3	–
5c	149.7	127.6	140.2	125.7	131.0	146.7	171.5	45.2	31.8	19.8	13.1	42.9	30.1	19.8	12.9	116.4	123.6	–

s = resonances coming from the less abundant *syn* form for **2a**, **2b**, **3a** and **3b,** respectively. Complexes **4a**, **4b**, **5a** and **5b** are only in the *syn–anti* conformation.

with their N-geminal group. Analogously, resonance assignments of the dialkyl complexes are mainly supported by the space contacts detected between the *internal* N–H and both the geminal *syn* and the *anti* α-alkyl protons; the *external* N–H shows a single dipolar coupling toward the *anti* α-alkyl protons (Schemes 1–3).

Comprehensive structural deductions and unambiguous signal assignments have been achieved by the combined use of 2D-TOCSY, 2D-NOESY, ^{13}C-HSQC, ^{13}C-HMBC and ^{15}N-HSQC (Tables 3 and 4). Spectra performed down to 200 K for the metal complexes do not show further resonance splits, suggesting a low rotational

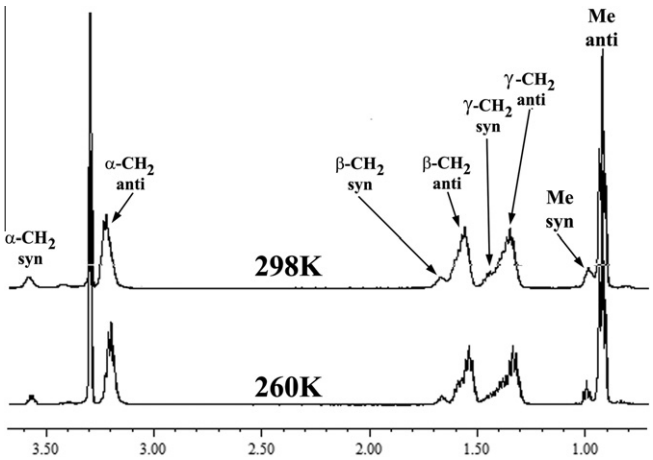

Fig. 4. Alkylic region of the ^{1}H NMR spectra at 260 and 298 K with signal assignment for the complex $[Pd(bipy)(n\text{-}buTU)_2]Cl_2$ **3a** in CD_3OH.

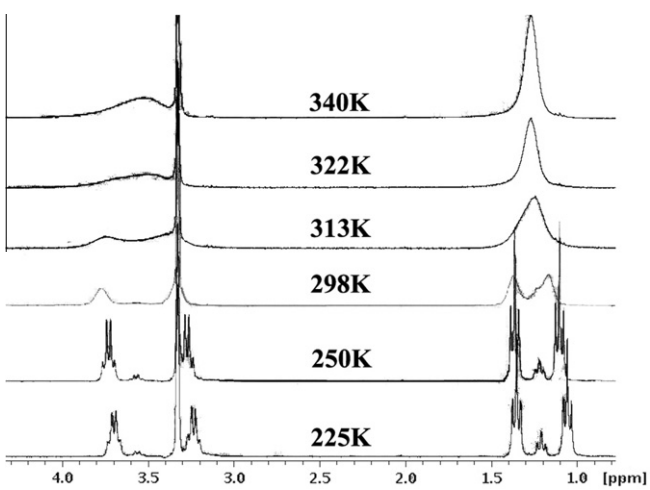

Fig. 5. Variable temperature spectrum, expanded in the ethyl region, for the complex $[Pd(bipy)(dietTU)_2]Cl_2$ **4a** in CD_3OH.

barrier about the M–S and/or S–C bonds. A significant consequence of the metal coordination is a conformational selection. Metal coordination stabilizes the *anti*-form of the monoalkyl ligands and the *syn–anti* arrangement of the dialkyl ligands exclusively selected as *syn–anti* conformers (Tables 3 and 4, and Experimental Section). The enhancement of the C–N double bond character is supported by the overall cs analyses. The ^{15}N resonances are weakly deshielded by coordination, while the $^{13}C{=}S$ resonances are shielded. This is consistent with the metal electron withdrawing being balanced by a mesomeric shift of the N atom lone pair toward C=S. Moreover, all of the ^{1}H and ^{13}C resonances of the N-alkyl groups are shifted to higher frequencies; this effect fades out by increasing the distance from the N atom. Comparative cs analysis of the bidentate ancillary ligands, shows *phen* has a stronger electron withdrawing effect with respect to *bipy*.

All the complexes, in accord with the NMR evidences, behave in water and methanol as 1:2 electrolytes (Table 6). The double positive cations show a moderate acidic character. Titrations monitored by a pH-meter in water, with standard NaOH titrating solutions at ionic strength $I = 10$ mmol dm^3 ($NaNO_3$), showed pKa values ranging from 3.8 to 4.2. Since in water/acetone-d_6 (80:20 v:v), up to pH = 7, the N–H signals are entirely preserved, we attribute the acidity to hydrolytic pathways of the double-positively charged complexes [26].

3.3. Comparative thermodynamic analysis of C–N rotation

Table 5 reports comparative $\Delta G^{\#}$ values for rotation around the C–N bond for all of the presented compounds **1**–**5**, **1a**–**5a** and **1b**–**5b**. According to the experimental data, rotation about C–N of thioureas is an asynchronous process which takes place, in principle, with different rates referred to the two amino-groups, influenced by either steric and electronic effects. Taking the activation energy of **1** ($\Delta G^{\#}$ = 54 kJ/mol) as a reference, the introduction of an alkyl substituent (**2** and **3**) causes an increment of about 12 kJ/mol referred to the C–NHR rotation; whereas the neighboring C–NH_2 is affected by a $\Delta G^{\#}$ decrement of about 8 kJ/mol in the case of the *syn* conformer. The $\Delta G^{\#}$ differences are reasonably due to the electron pushing action of the alkyl group which causes asymmetric sharing of the C–N double bond character along the two amino branches. The steric influence of the alkyl group in **2** and **3** is clearly evidenced by the lower C–NH_2 rotational barrier of the *syn* isomer (47–48 kJ/mol) respect to the *anti*-form, hampered by the internal alkyl substituent (55–57 kJ/mol).

Dialkyl thioureas **4** and **5** show a significant decrease of the C–NHR rotational barrier ($\Delta G^{\#}$ = 53–55 kJ/mol) with respect to **2** and **3**. This can be interpreted on the basis of an equal distribution of the double bond character between the two symmetric amino branches. Beyond the forced symmetric sharing of the double bond character, for **4** and **5** the 10 kJ/mol decrease of the rotational barrier is likely due to the destabilization of the ground states because of alkyl overcrowding.

Metal coordination through the S atom decreases the C=S double bond character [27], prompting the C–N bonds toward a greater double bond character. As a consequence mono-alkyl complexes show a $\Delta G^{\#}$ increase of about 5 kJ/mol for C–NHR and 4 kJ/mol for C–NH_2. Di-alkyl thioureas display, upon coordination, a more important (10 kJ/mol) increase of the C–NHR rotational barrier. This should be caused by a more rigid framework imposed by the metal to the overcrowded di-alkyl structures.

4. Conclusions

This paper report the specific dynamic behavior of 10 Pd^{II} complexes with substituted thioureas. Variable temperature NMR experiments, joined to many different techniques of homo-nuclear and hetero-nuclear spectroscopy, enabled us to shed light on the conformations and dynamic behavior of these species. Conformational isomers are generated by hampered rotation about the C–N bond: alkyl groups on the same side (*syn*) or on the other side (*anti*) respect to the S atom give rise to different NMR signals whose dynamic connection is proved by the mutual chemical exchange. Both for the N-mono-alkyl and the symmetric N,N′-dialkyl species the stability of the conformational isomers is solvent dependent.

Experimental data concerning the Pd^{II} thioureate complexes testify: (a) hindered C–N rotation (Figs. 4 and 5, and Table 5); (b) free rotation about the C–S and S–Pd bonds down to 200 K; (c) drastic conformational selection (similar but stronger than the one observed for the free species in chloroform) leaving mostly the *syn* form for the monoalkyl substrates (Fig. 4 and Experimental Section) and exclusively the *syn–anti* adduct for the dialkyl ligands (Fig. 5 and Experimental Section). NMR analysis of the Pd^{II} complexes, which are also good candidates for biological activity against cancer cells, supports a mesomeric increase of the C–N double bond character, in spite of the decrease of the C–S double bond character. This report, concerning the solution structure of Pd^{II} complexes, is a possible sound starting point for further biochemical studies.

Table 5
Activation free energy for C–N rotation ($\Delta G^{\#}$ in kJ/mol), at coalescence temperature (range 250–340 K), for compounds **1**–**5**, **1a**–**5a** and **1b**–**5b**.

Mono alkyl compounds	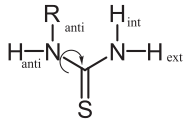	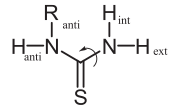	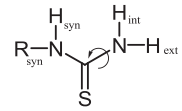
1	–	–	54 (275 K)
1a	–	–	59 (305 K)
1b	–	–	59 (310 K)
2	64 (316 K)	57 (305 K)	47 (236 K)
2a	68 (328 K)	60 (308 K)	–
2b	68 (315–330 K)	60 (305)	–
3	64 (320 K)	55(270 K)	48(247 K)
3a	67 (335 K)	60 (308 K)	–
3b	67 (338 K)	60 (310 K)	–
Dialkyl compounds	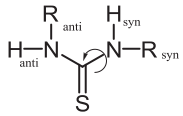		
4	53 (275 K)	–	–
4a	64 (318 K)	–	–
4b	64 (320 K)	–	–
5	55 (285 K)	–	–
5a	63 (316 K)	–	–
5b	64 (324 K)	–	–

Coalescence temperatures in brackets. The $\Delta G^{\#}$ values measured by different coalescences show weak temperature dependence.

Table 6
Equivalent conductivity ($Ohm^{-1}\ cm^2\ mol^{-1}$) for the studied complexes in CH_3OH.

Complex	Molar concentration	Equivalent conductivity
1a	1.58×10^{-3}	159.4
1b	1.10×10^{-3}	167.6
2a	1.56×10^{-3}	149.1
2b	1.28×10^{-3}	158.3
3a	1.25×10^{-3}	162.8
3b	1.53×10^{-3}	151.0
4a	1.08×10^{-3}	132.8
4b	1.11×10^{-3}	151.0
5a	1.07×10^{-3}	128.2
5b	1.06×10^{-3}	148.0

Acknowledgement

We are grateful to "Il Ministero della Ricerca Scientifica" for the financial support of our research programs.

Appendix A. Supplementary data

The supplementary material reports variable temperature stack-plot for the presented compounds. Supplementary data associated with this article can be found, in the online version, at http://dx.doi.org/10.1016/j.poly.2012.07.064.

References

[1] M.G. Fisher, P.A. Gale, M.E. Light, R. Quesada, CrystEngComm 10 (2008) 1180.
[2] S. Nadeem, M.K. Rauf, M. Bolte, S. Ahmad, S.A. Tirmizi, M. Asma, A. Hameed, Trans. Met. Chem. 35 (2010) 555.
[3] P.A. Gale, M.E. Light, R. Quesada, CrystEngComm 8 (2006) 178.
[4] P.A. Gale, M.E. Light, R. Quesada, Chem. Commun. 7 (2005) 5864.
[5] S.-T. Cheng, E. Doxiadi, R. Vilar, A.J.P. White, D.J. Williams, J. Chem. Soc., Dalton Trans. (2001) 2239.
[6] P. Diaz, D.M.P. Mingos, R. Vilar, A.J.P. White, D.J. Williams, Inorg. Chem. 43 (2004) 7597.
[7] (a) E. Wong, C.M. Giandomenico, Chem. Rev. 99 (1999) 2451;
(b) Y. Jung, S.J. Lippard, Chem. Rev. 107 (2007) 1387.
[8] J. Reedijk, Chem. Rev. 99 (1999) 2499.
[9] J. Kozelka, F. Legendre, F. Reeder, J.-C. Chottard, Coord. Chem. Rev. 61 (1999) 190.
[10] R.T. Dorr, Platinum and other metal coordination compounds in cancer chemotherapy, in: H.M. Pinedo, J.H. Schornagel (Eds.), Plenum, New York, 1996, pp. 131–154.
[11] M. Bloemink, J. Reedijk, in: A. Sigel, H. Sigel (Eds.), Metal Ions in Biological Systems, Marcel Dekker, vol. 32, New York, 1996.
[12] K.A. Mitchell, C.M. Jensen, Inorg. Chim. Acta 265 (1997) 103.
[13] O. Wernberg, J. Chem. Soc., Dalton Trans. (1986) 725.
[14] N. Summa, W. Schiessl, R. Puchta, N. van Eikema Hommes, R. van Eldik, Inorg. Chem. 45 (2006) 2948.
[15] Ž.D. Bugarčič, G. Liehr, R. van Eldik, J. Chem. Soc., Dalton Trans. (2002) 2825.
[16] S. Mallick, S. Mondal, B.K. Bera, P. Karmakar, S.C. Moi, A.K. Ghosh, Transition Met. Chem. 35 (2010) 469.
[17] Y.-S. Wu, Klaus.R. Koch, V.R. Abratt, H.H. Klump, Arch. Biochem. Biophys. 440 (2005) 28.
[18] A.R. Kheradi, G. Saluta, G.L. Kucera, C.S. Day, U. Bierbach, Bioorg. Med. Chem. Lett. 19 (2009) 3423.
[19] G. Marverti, M. Cusumano, A. Ligabue, M.L. Di Pietro, P.A. Vainiglia, A. Ferrari, M. Bergomi, M.S. Moruzzi, C. Frassineti, J. Inorg. Biochem. 102 (2008) 699.
[20] M. Cusumano, M.L. Di Pietro, A. Giannetto, P.A. Vainiglia, J. Inorg. Biochem. 99 (2005) 560.
[21] C. Vetter, C. Wagner, J. Schmidt, D. Steinborn, Inorg. Chim. Acta 359 (2006) 4326.
[22] C. Vetter, C. Wagner, G.N. Kaluderović, R. Paschke, D. Steinborn, Inorg. Chim. Acta 362 (2009) 189.
[23] C. Vetter, G.N. Kaluderović, R. Paschke, R. Kluge, J. Schmidt, D. Steinborn, Inorg. Chim. Acta 363 (2010) 2452.
[24] J. Sandstrom, Dynamic NMR Spectroscopy, Academic Press Inc. Ltd., London, 1982. pp. 80–81.
[25] (a) S. Nadeem, M.K. Rauf, S. Ahmad, M. Ebihara, S.A. Tirmizi, S.A. Bashir, A. Badshah, Transition Met. Chem. 34 (2009) 197;
(b) S. Nadeem, M.K. Rauf, S. Ahmad, M. Ebihara, S.A. Tirmizi, S.A. Bashir, A. Badshah, Transition Met. Chem. 35 (2010) 555.
[26] G. Arena, A. Gianguzza, L. Pellerito, R. Purrello, E. Rizzarelli, J. Chem. Soc., Dalton Trans. 1234 (1990) 2603.
[27] (a) L. Perez-Marin, M. Castro, E. Otazo-Sanchez, G.A. Cisneros, Int. J. Quantum Chem. 80 (4/5) (2000) 609;
(b) M.A. Nabar, Bull. Chem. Soc. Jpn. 39 (5) (1966) 1067;
(c) A.N. Sergeeva, L.A. Kiseleva, S.M. Galitskaya, Zh. Neorg. Khim. 16 (7) (1971) 1782;
(d) V.I. Baranovskii, N. Yu, N.S. Kukushkin, V. Panina, V. Sibirskaya, Koord. Khim. 3 (11) (1977) 1732.